Available online at www.sciencedirect.com
SCIENCE DIRECT®
PERGAMON
Continental Shelf Research 23 (2003) 125–144
CONTINENTAL SHELF RESEARCH
www.elsevier.com/locate/csr

Seasonal and interannual variation in the hydrography of the Cariaco Basin: implications for basin ventilation

Yrene Astor[a], Frank Muller-Karger[b,*], Mary I. Scranton[c]

[a] *Fundación La Salle de Ciencias Naturales, Estación de Investigaciones Marinas de Margarita, Apartado 144 Porlamar, Isla de Margarita, Venezuela*
[b] *College of Marine Science, University of South Florida, St. Petersburg, FL 33701, USA*
[c] *Marine Sciences Research Center, State University of New York, Stony Brook, NY 11794-5000, USA*

Received 28 September 2001; accepted 12 March 2002

Abstract

The hydrography of the Cariaco Basin (temperature, salinity, density, dissolved oxygen concentration) was studied using monthly observations collected between November 1995 and August 1998 at the CArbon Retention In A Colored Ocean (CARIACO) time-series station (10.5°N, 64.66°W). Satellite scatterometer wind estimates showed that changes in the wind preceded changes in hydrography by 1–2 weeks. Upward migration of isopleths within the upper 150 m was observed between November and May each year, when the Trade Wind was more intense. A seasonal deepening of the isopleths was observed when winds relaxed. A secondary upwelling event was observed every year between July and August, in response to an intensification of the southward component of the Trade Wind. Interannual variation in the upwelling cycle was driven in part by variations in wind intensity and in part by other events at time scales of 1–3 months. The latter were associated with 90–140 m deep intrusions of Caribbean Sea water that forced waters above them to the surface. Satellite-derived sea surface height anomaly maps demonstrated that these events were related to cyclonic and anticyclonic eddies moving along the continental shelf. Waters deeper than 1200 m showed small temperature and salinity increases of $0.0075^{\circ}C\,yr^{-1}$ and $0.0016\,yr^{-1}$, consistent with previous estimates.

Keywords: Upwelling; Hydrography; Ventilation; Anoxic; Time series; Eddies; Altimetry

1. Introduction

The Cariaco Basin is a 1400 m deep depression within the continental shelf of Venezuela (Fig. 1), connected to the southeastern Caribbean Sea across a sill that reaches approximately 140 m at its deepest point. A detailed record of annual to decadal scale climate change is stored in the sediments of this Basin. The sediment record, which spans over 100,000 yr, provides one of the longest and most accurate logs of past climate change in the tropical ocean. Variation in sedimentation rates have been linked to past variation in regional fluvial discharge, local upwelling intensity, Trade Wind intensity, position of the Intertropical Convergence Zone, and water mass formation in the North Atlantic (Peterson et al.,

*Corresponding author.
E-mail addresses: edimar_biomarina@unete.com.ve (Y. Astor), carib@marine.usf.edu (F. Muller-Karger), mscranton@notes.cc.sunysb.edu (M.I. Scranton).

0278-4343/03/$ - see front matter
PII: S0278-4343(02)00130-9

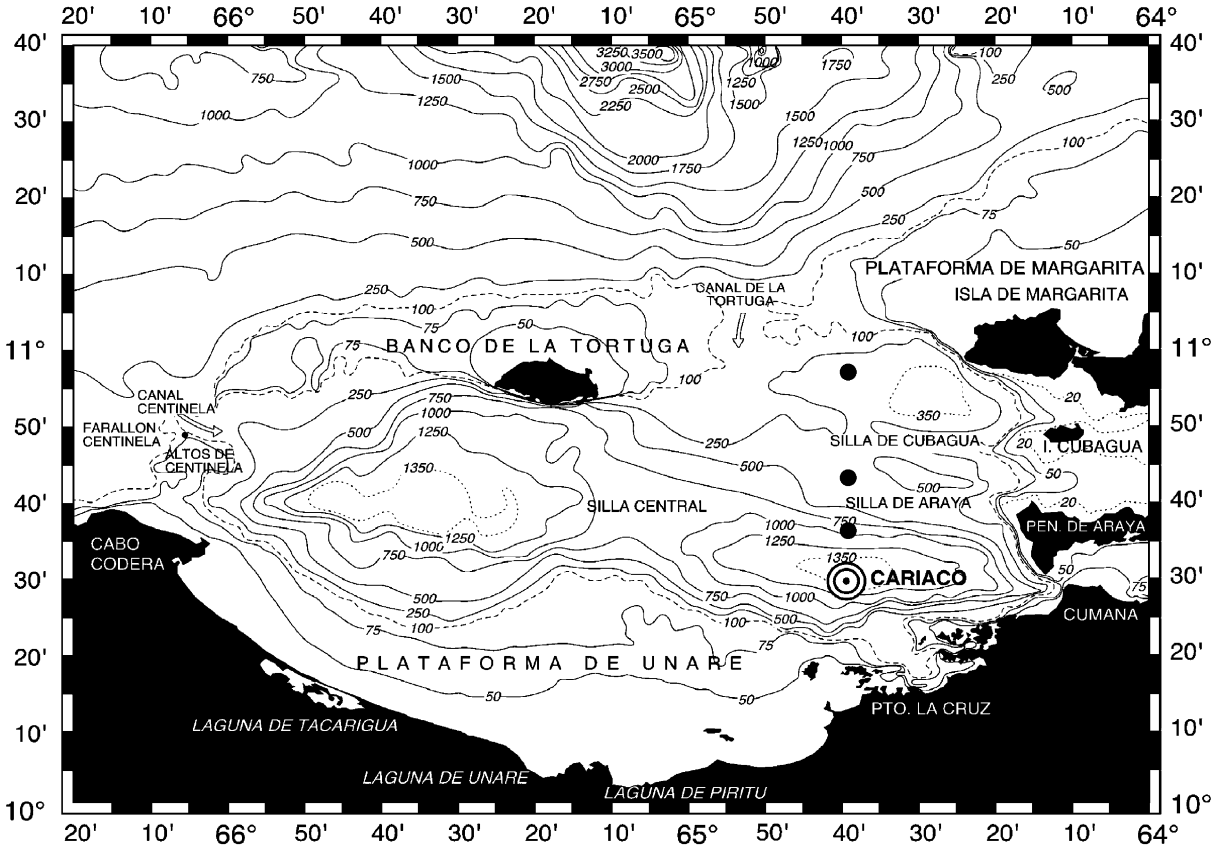

Fig. 1. The Cariaco Basin showing location of the CARIACO station (open circle) and monthly XBT stations (filled circles).

1991; Hughen et al., 1996; Hughen et al., 1998; Haug et al., 1998; Black et al., 1999).

To fully understand the climate record as stored in the sediments of the Cariaco Basin, it is necessary to understand the hydrography of the water column. This basin exhibits marked seasonal changes in hydrography within the upper 150 m as a result of fluctuations in coastal upwelling and the lateral advection of Caribbean water masses (Astor et al., 1998). In the past, it has been difficult to reconstruct the controls on the hydrography of waters shallower than 300 m because oceanographic observations were sporadic and infrequent. Deeper waters in the basin typically experience relatively slow change in chemical and physical properties (Scranton et al., 1987; Zhang and Millero, 1993; Scranton et al., 2001). Occasionally, sudden changes in the chemistry and turbidity of deep waters occur due to cataclysmic events such as earthquakes (Zhang and Millero, 1993; Thunell et al., 1999; Scranton et al., 2001).

This study attempts to quantify the seasonal and interannual variation of the upwelling phenomenon and of intrusions of Caribbean Sea water into the basin. To accomplish this, we used a time series of observations collected between November 1995 and August 1998 under the CArbon Retention In A Colored Ocean (CARIACO) Program (Muller-Karger et al., 2000).

2. Methods

Monthly cruises were conducted to the CARIACO station (10.5°N, 64.66°W; Fig. 1) aboard the R/V *Hermano Ginés* of the Fundación La Salle

de Ciencias Naturales de Venezuela. During each cruise, five to six hydrocasts were performed to collect water samples at 20 depths between the surface and 1310 m. Continuous profiles of temperature and salinity were collected using a SeaBird CTD. Between November 1995 and September 1996, three separate SBE-19 CTDs were used in repeated casts until a reliable salinity profile was obtained below the oxycline. The SBE-19 model CTDs frequently failed to provide reliable conductivity values below the oxycline in the Cariaco Basin. Starting in September 1996, the SBE-19 CTDs were replaced by an SBE-25 CTD, which provided extremely accurate and reliable data in anoxic waters. All CTDs were calibrated at the SeaBird factory once per year.

Continuous salinity profiles were calculated from the CTD measurements. Discrete salinity samples were analyzed using a Guildline Portasal 8410 salinometer calibrated with IAPSO Standard Seawater, with a precision of better than ± 0.003. These salinity values were used to check, and when necessary calibrate, the CTD salinity profiles.

Continuous dissolved oxygen (O_2) profiles were obtained with a YSI 23-Y sensor coupled to the SBE-25 CTD. Discrete oxygen samples were collected in duplicate using glass-stoppered bottles and analyzed by Winkler titration (Strickland and Parsons, 1972, as modified by Aminot, 1983). The analytical precision for discrete oxygen analysis was $\pm 3\,\mu M$, based on analysis of duplicate samples, with a detection limit of $5\,\mu M$.

The pH samples were collected directly in a 10 cm cell and analyzed on board following the spectrophotometric procedure described by Clayton and Byrne (1993). Samples for nitrite and nitrate were collected in plastic bottles, filtered through a $0.7\,\mu M$ filter within minutes of collection and frozen in plastic bottles until analysis at either the Universidad de Oriente (Cumana, Venezuela) or the University of South Florida (USF). The analyses followed the standard techniques described by Strickland and Parsons (1972). USF follows the recommendations of Gordon et al. (1993) for the WOCE WHP project for nutrient analysis.

Starting in September 1997, expendable bathythermographs (XBT) were launched monthly at pre-established locations (Fig. 1) using a Sippican MK12 oceanographic data-acquisition systems (ODAS). The objective was to assess spatial variation in the distribution of water masses around the CARIACO station in the upper 200 m.

A detailed sea surface temperature (SST) time series was derived from daily images of the NOAA Advanced Very High-Resolution Radiometer (AVHRR) satellite sensors covering the CARIACO station. Data were collected using the high-resolution picture transmission antenna located at the University of South Florida, in St. Petersburg, FL (http://imars.marine.usf.edu). Passes from all NOAA-AVHRR sensors were combined in order to build the time series (nighttime and daytime passes from the NOAA 11 through 14 satellites). SST was computed using the multi-channel sea-surface temperature (MCSST) algorithm developed by McClain et al. (1983). The approximate root mean square error of the AVHRR SST retrievals, confirmed in this study through comparisons with in situ data, is of the order of 0.5°C. Local time series of SST were constructed by averaging all observations within a box of approximately $12\,km^2$ for each image.

There are no direct wind observations within the Cariaco Basin. Therefore, in order to assess the effect of the wind, we examined wind measurements from two locations on nearby Margarita Island and also wind estimates derived by satellite remote sensing. Specifically, we used wind records from Santiago Mariño Airport (10°54′N, 63°57.6′W) and from the Fundacion La Salle's Estacion de Investigaciones Marinas de Margarita (EDIMAR) at Punta de Piedras (10°54′N, 64°12′W). These stations are only 26 km apart on Margarita Island, and both are approximately 80 km to the northeast of the CARIACO station. The airport data are the official wind data for Margarita Island, and are archived and distributed by the Venezuelan Airforce (*Fuerza Aerea de Venezuela*). Hourly winds were averaged to daily values for each station.

Wind speed and direction estimates for the southern Caribbean Sea were also derived from satellite sensors. The data were collected by the Active Microwave Instrument (AMI)

scatterometer on the European Remote-Sensing Satellites 1 and 2 (ERS-1 and ERS2) and by the NASA scatterometer flown on the Japanese ADEOS-I satellite. The data were processed by the French Centre ERS d'Archivage et de Traitement at French Ocean Research Institute at $1^\circ \times 1^\circ$ resolution (Pouliquen et al., 1996). We extracted the north–south (meridional) and east–west (zonal) wind velocity components at 12.5°N, 64.5°W, i.e. immediately to the north of the Cariaco Basin.

A time series of Sea Surface Height (SSH) anomaly images derived from satellite data collected during 1997–1998 were used to study sea-level variations associated with eddies north of the Venezuelan continental shelf. The SSH anomaly data were obtained from the Naval Oceanographic Office (NAVO) at the Stennis Space Center, Mississippi. The NAVO Modular Ocean Data Assimilation System (MODAS) product is derived from the Geosat follow-on, TOPEX/Poseidon, and the ERS-2 altimeter satellites. The product represents geopotential anomaly of the sea surface in dynamic meters relative to an assumed zero geopotential anomaly at 1000 or 500 dbar. NAVO combined the MODAS optimally interpolated sea surface height deviation and the MODAS climatological mean geopotential anomaly. The optimum interpolation schemes were described at the NAVO Internet website (http://www7300.nrlssc.navy.mil/altimetry/). Only data since January 1997 were available through this source. Observations for 1996, based solely on coarser grid resolution TOPEX measurements, were obtained from NASA's Jet Propulsion Lab's Ocean Earth Science Information Partner Federation (Victor Zlotnicki and Akiko Hayashi, personal communication; http://oceanesip.jpl.nasa.gov/sealevel/along.shtml).

3. Results

3.1. The wind

Substantial differences exist between the various wind time series. Of particular concern were the observations that the airport's anemometer provided poor resolution of north–south wind direction, that it showed a marked phase difference relative to both the EDIMAR station and the scatterometer winds, and that it showed a trend toward increasing wind speed with time which was not detected in the other two series. This suggested that the airport device had mechanical problems. In this study we use the scatterometer series to examine forcing of hydrographic variability because this wind series covers the period of interest and is reasonably well validated by the EDIMAR station (Fig. 2).

The wind was predominantly westward at all times and followed a marked seasonal cycle (Fig. 2). Seasonal minima in the scalar wind speed ($<6\,\mathrm{m\,s^{-1}}$) occurred between approximately July and November. Seasonal maxima ($>7\,\mathrm{m\,s^{-1}}$) occurred between February and May–June. A periodogram confirmed that the strongest signal was the annual cycle (Fig. 3), but both the scalar and zonal wind components (u) also showed energy peaks at 6 and 2.5 month frequencies. The only clear signal of the meridional wind component (v) was the annual signal.

The seasonal increase in wind speed started in October, November or December depending on the year (Fig. 2). In early 1997, stronger winds were observed relative to winds during the same period in 1996 and 1998. Weaker winds ($<5\,\mathrm{m\,s^{-1}}$) were observed between about July and September–October. In 1998, substantial weakening in the wind started as early as April, and winds seemed more variable than in other years.

The meridional (north–south) component of the wind (v; range -3 to $1\,\mathrm{m\,s^{-1}}$) was weaker than the zonal wind but it showed a strong seasonal and interannual variation. The wind turned slightly to the south during October–December, when the Trade Wind intensified, and turned again more to the west when winds weakened. There was an episode of stronger southward v in January 1997 (Fig. 2). No seasonal variation and very weak meridional winds were observed in 1998.

A cross-correlation analysis between satellite-derived SST (Fig. 2) and scalar wind intensity shows maximum correlation at a positive lag of 1–2 weeks (Fig. 4). This demonstrated that

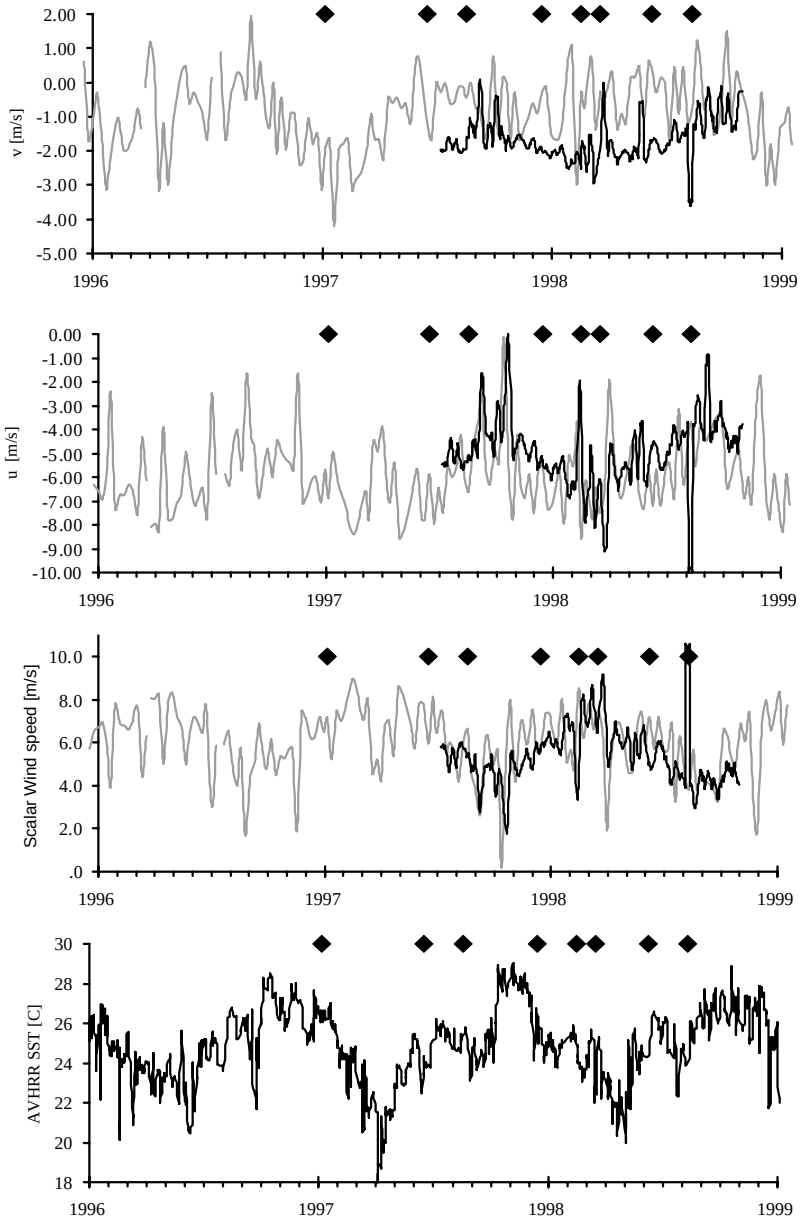

Fig. 2. Wind speed ($m\,s^{-1}$) and sea surface temperature series. Scatterometer (gray line) and EDIMAR anemometer winds (solid line), with meridional component (v, top panel), zonal component (u; second panel from top), and scalar wind speed (third panel). Satellite-derived AVHRR SST over the CARIACO site shown in bottom panel. Diamonds show subsurface ventilation events in the Cariaco Basin (Table 1).

changes in the wind preceded changes in SST by a few days, showing that prior conclusions based on airport winds (Muller-Karger et al., 2000, 2001), are incorrect.

3.2. The hydrography

The hydrography of Cariaco Basin waters varied in different ways depending on depth

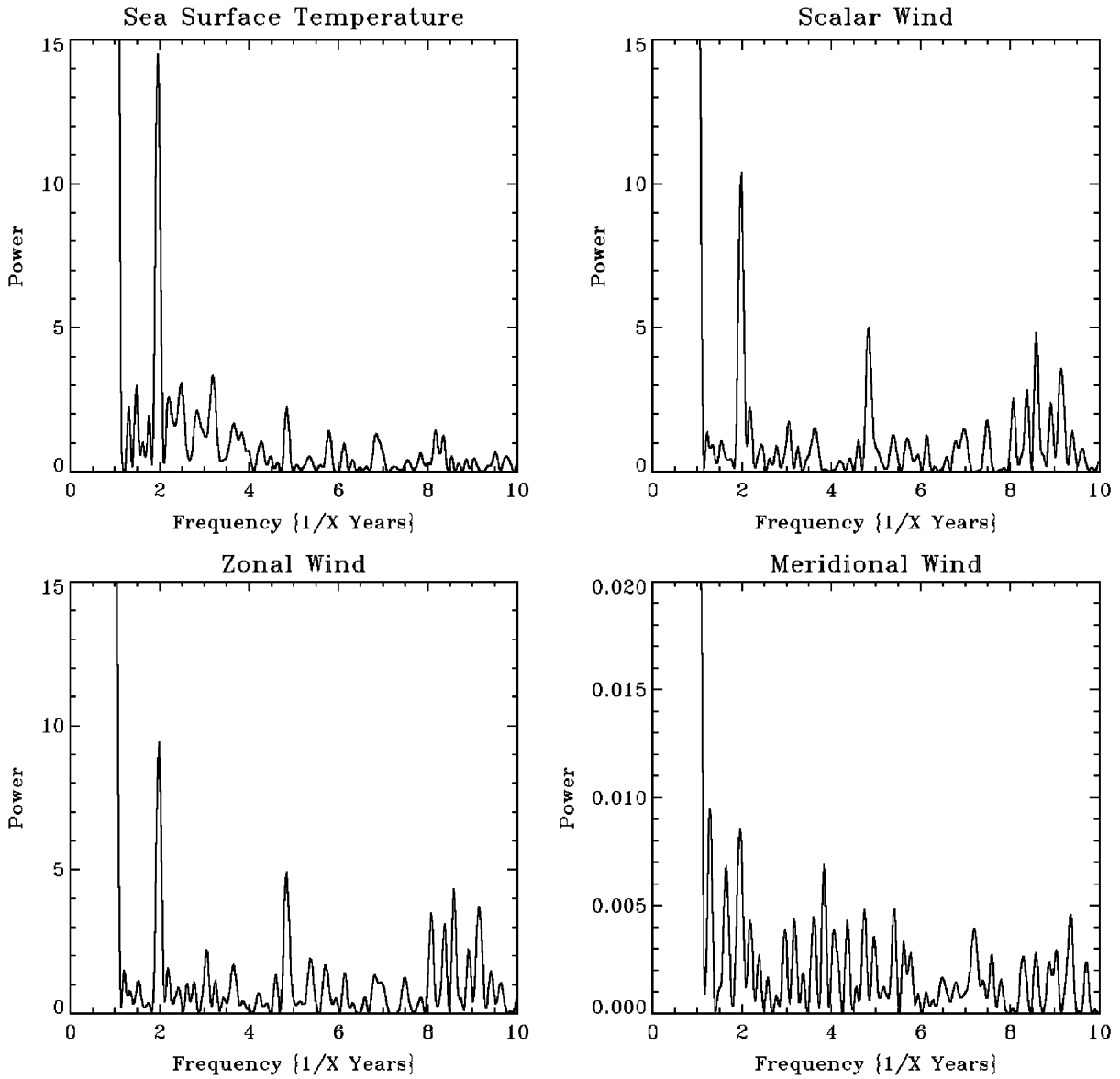

Fig. 3. Periodogram showing frequencies at which maximum periodic energy was observed in the AVHRR SST series and the scalar, u and v components of the scatterometer wind series. Periods at which energy peaks occur are estimated by dividing 1 (a year) by the appropriate number in the abscissa.

(Fig. 5). Waters shallower than 200 m showed marked temporal variation. Changes in sea surface temperature (SST; Fig. 2) and the vertical excursions of the 21°C isotherm (Fig. 5a) were used to define periods of upwelling or of upwelling relaxation. Upwelling was defined as the upward displacement of isotherms between consecutive sampling periods, and upwelling relaxation as the apparent downward migration of isotherms. In general, upwelling started in November or December and subsided sometime after the first quarter of the following year. The 21°C isotherm migrated between 130 m and about 20 m, reaching its shallowest depth approximately in April. The

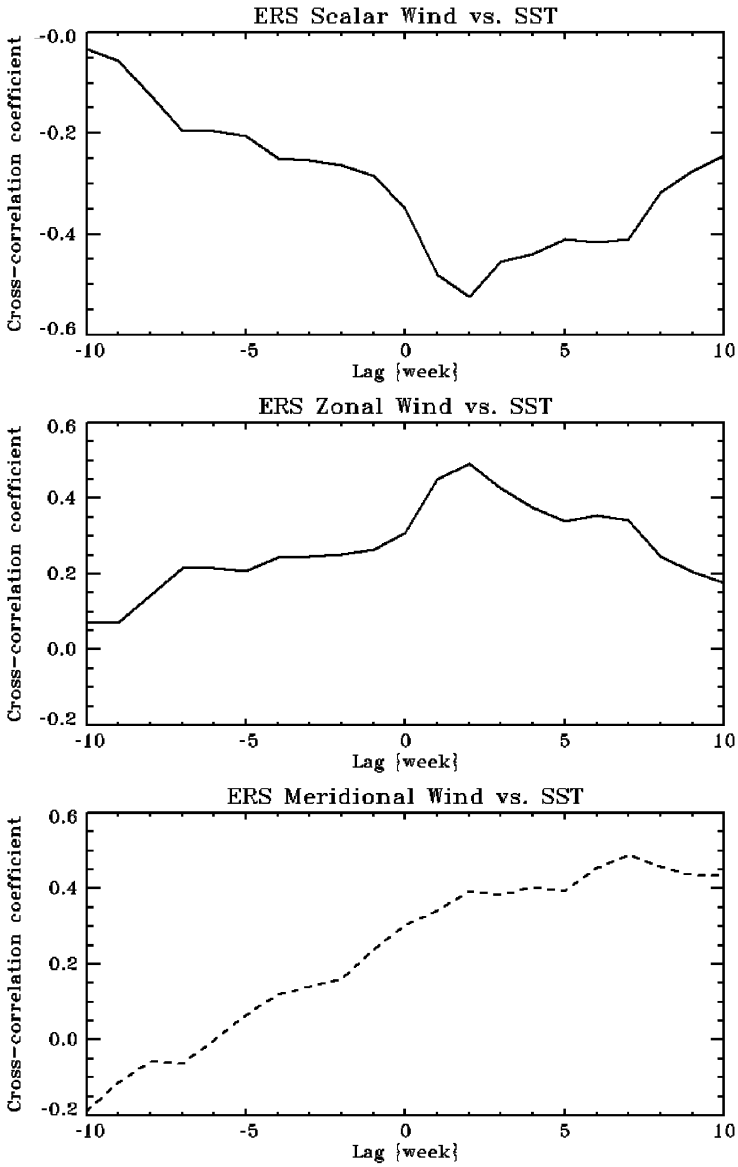

Fig. 4. Lagged cross-correlation analyses between scatterometer wind and SST, with lags measured in weeks. From top to bottom: scalar wind, u (zonal), and v (meridional) winds and SST. Negative lags indicate wind lagged the SST.

23°C isotherm reached the surface in February 1996, and SST lower than 23°C was observed through March. Similar conditions were observed in 1997. In both 1996 and 1997, isotherms migrated downward after April, and reached their deepest levels between September and October. The 1997–1998 season showed a more irregular pattern in the vertical motion of isotherms. While the 23°C isotherm rose toward the surface in late 1997, it reached the surface only briefly in March 1998.

A secondary upwelling episode lasting only about a month was observed in July–August each year. This feature, first detected in the annual SST

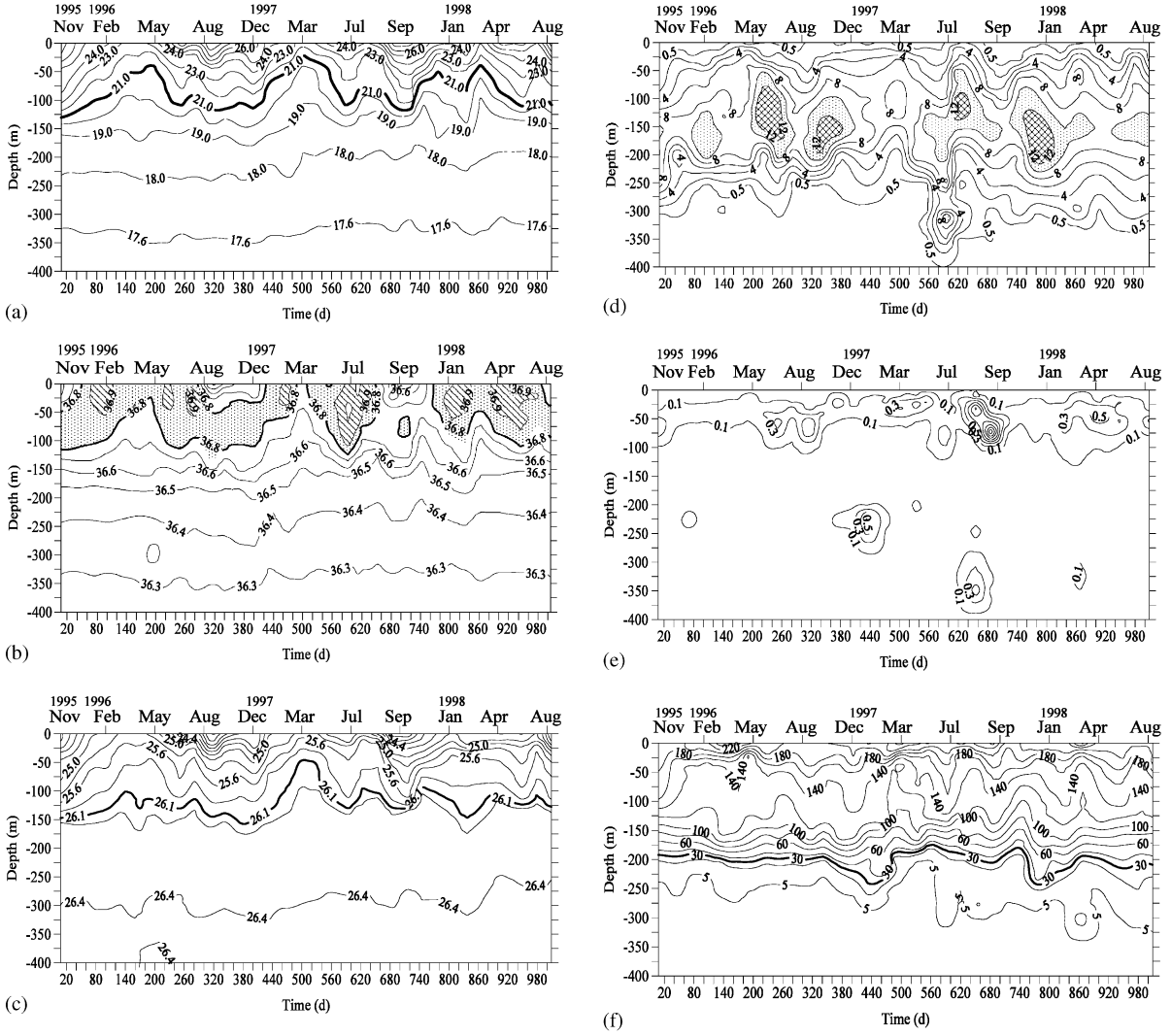

Fig. 5. (a) Temperature (°C), (b) salinity (with maxima tracing the subtropical underwater shaded), (c) sigma-t, and (d) nitrate (μM), (e) Nitrite (μM), and (f) dissolved oxygen (μM) variations at the CARIACO time-series station between November 1995–August 1998.

cycle (Fig. 2), was more noticeable in the behavior of the 21°C isotherm below the surface (Fig. 5a). This feature is responsible for the semiannual peak in the SST periodogram (Fig. 3). The 21°C isotherm migrated as much as 50 m toward the surface during this event. The strength of this secondary upwelling event varied, with 1997 showing the most pronounced and coldest event (SST = 24°C). Fig. 2 suggests that the mid-summer upwelling was related to the initiation of the southward turn in the Trade Wind.

Surface salinity at the CARIACO station changed seasonally, from greater than 36.8 in January–July to less than 36.6 between August and November (Fig. 5b). The surface salinity minima occurred during the rainy season (August–October). Large variations occurred in the depth of the salinity maximum (> 36.8), reflecting

changes in the depth of subtropical underwater (SUW; Wust, 1964; Morrison and Smith, 1990). While the SUW core was observed between 50 and 120 m during non-upwelling periods, it and sometimes waters located below it, reached the surface during upwelling.

The density structure of waters in the upper 150 m reflected the seasonal cycle of salinity and temperature (Fig. 5c). At the base of this layer, sigma-t (σ_t) was approximately constant at 26.20. The lowest σ_t values were observed at the surface during the rainy season (August–October), when the strongest stratification occurred between the surface and 150 m (a difference of about $2.9\sigma_t$ units). During the dry and windy season (February–May), the vertical density gradient weakened, with a difference of $0.8\sigma_t$ units between the surface and 150 m. Density increased slowly with depth below 150 m, reaching σ_t values of about 26.40 at 300 m. Density contrast in the deep waters is extremely small with the difference between sigma-theta at 550 m ($\sigma_\theta = 26.462$) and 1310 m ($\sigma_\theta = 26.474$) being only 0.012.

Waters in Cariaco above sill depth interacted with the open sea, but vertical mixing was inhibited by a strong pycnocline that started at the surface and extended to sill depth. Below 200 m, a muted advective regime was found where vertical temperature gradients were small and did not show a seasonal cycle. Waters deeper than 1200 m showed a small temperature increase over time, measurable only over many years of observation. Scranton et al. (1987) reported a potential temperature of 16.825°C below 1200 m in 1982. In November 1995, the potential temperature at this depth was 16.922°C. The increase of 0.097°C between 1982 and 1995 suggested a warming rate of $0.0075°C\,yr^{-1}$, in agreement with the previous estimate of Scranton et al. (1987). Similarly, an increase in salinity of 0.021 was observed below 1200 m between 1982 (36.204) and 1995 (36.225 ± 0.003). This is an increase of $0.0016\,yr^{-1}$, compared with $0.0009\,yr^{-1}$ estimated by Scranton et al. (1987). Considering that the instrumental precision for salinity is ± 0.003, there is close agreement between these estimates.

Nitrate concentrations (Fig. 5d) increased with depth to maxima of 10–12 μM between 100 and 200 m. Nitrate then decreased and disappeared between 300 and 400 m. The nitrate-containing zone extended to greater depths after June 1997, associated with an increase in depth of the oxic/anoxic interface. The primary nitrite maximum was found near 40 m (Fig. 5e) with nitrite disappearing between 50 and 100 m. A secondary nitrite maximum was observed in January and August 1997 (225 and 350 m, respectively) and in March 1998 (340 m).

Dissolved oxygen (O_2) concentrations followed a distinct seasonal cycle in the upper water column, with the highest values (>220 μM) observed in the upper 20 m in spring (usually March; Fig. 5f). For the temperature and salinity of the SUW, O_2 saturation is expected to lie between 196 and 216 μM. However, values exceeding 270 μM were observed in this water mass at the CARIACO station during the upwelling period. The lowest surface values (190–200 μM) were typically observed between August and November.

Both the YSI probe and discrete O_2 samples showed that O_2 concentrations decreased with depth and typically became undetectable below 250–320 m (Figs. 5f, 6 and 7). Because of problems with probe calibration and probe drift, we used the

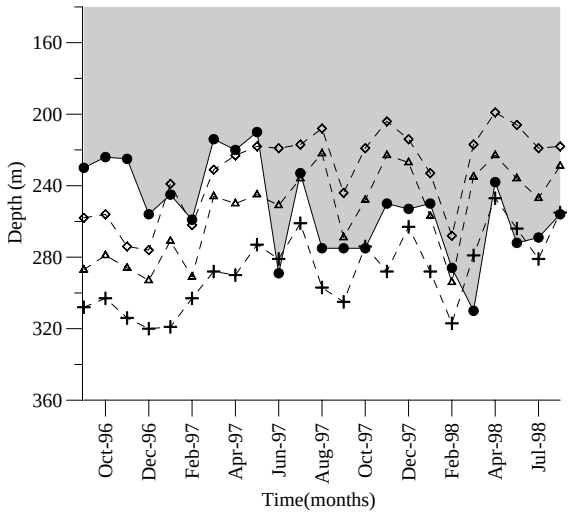

Fig. 6. Fluctuation in the depth of the oxic–anoxic interface (shaded area was defined by line connecting filled circles) and of selected density levels (σ_t): 26.38 (◇), 26.39 (△) and 26.40 (+), at the CARIACO time-series station between August 1996 and August 1998.

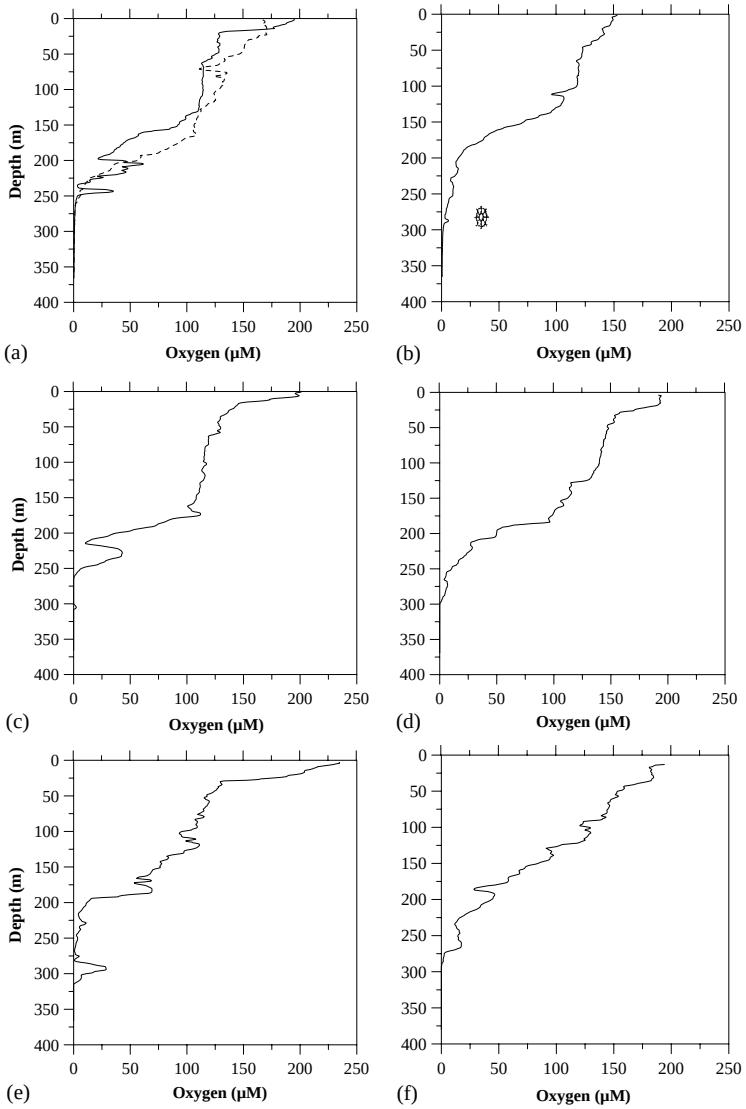

Fig. 7. Vertical distribution of O_2 (μM) at the CARIACO station in December 1996, showing normal conditions (----, a), and during selected ventilation events detected in 1997 and 1998: January 1997 (—, a), June 1997 (b), December 1997 (c), February 1998 (d), March 1998 (e), and June 1998 (f).

discrete samples (50 m sampling interval) to identify the depth at which oxygen vanished. The depth of the oxic–anoxic interface was defined as the depth where oxygen concentrations became undetectable ($<5\,\mu M$). In 1996, the interface was observed at about 225–250 m (Fig. 5f). Between December 1996 and January 1997, the $5\,\mu M$ O_2 isopleth sank to about 290 m and then rose again to about 200 m in May 1997. In June, the isopleth sank to almost 320 m, and remained deeper than 275 m through January 1998 (Figs. 5f and 6). It moved below 300 m in March 1998, then rose briefly to 250 m in April, then sank again in May to remain near 275 m through the rest of the observation period. Fluctuations in the depth of the interface seemed to be independent of variations in density. For example, there was no relationship with the depth of the $\sigma_t = 26.400$

horizon which was located near 300 m throughout the study period (Figs. 5c, 5f and 6).

The continuous O_2 profile generated using the YSI probe showed substantial variability at intermediate depths. Fig. 7 includes a "normal" O_2 vertical profile, obtained on December 14, 1996. It shows a relatively smooth decrease in O_2 concentration below 200 m. Fig. 7 also shows O_2 profiles when secondary oxygen maxima or a deepening of the oxic–anoxic interface were observed. At least eight such events were observed between 1997 and 1998. The secondary maxima were as large as 20–60 μM and typically were found in the 200–350 m depth intervals (Table 1). Discrete samples frequently missed such features because of our coarse depth sampling intervals.

4. Discussion

Because paleoceanographic studies seek to relate changes in the sediment record in the Cariaco Basin to cycles in surface hydrography and productivity, it is important to understand the timing, intensity, and variability of near-surface phenomena (Thunell et al., 2000; Muller-Karger et al., 2001). Upwelling in the Cariaco Basin has long been thought to occur in direct response to seasonal changes in the intensity of the Trade Wind (Richards and Vaccaro, 1956; Richards, 1960; Richards, 1975; Herrera and Febres-Ortega, 1975; Muller-Karger and Aparicio, 1994). Paleoceanographers have used this conceptual model to explain glacial to interglacial variations in the Cariaco sediment record as a consequence of climatic changes in wind intensity (Haug et al., 1998; Hughen et al., 1998; Black et al., 1999; Yarincik et al., 2000). Walsh et al. (1999) developed a numerical model based on this idea to examine the effect of single weeklong wind events on productivity and carbon flux. The CARIACO data generally confirm the relationship between wind events and upwelling, but they also show that other processes have significant influence on the strength and timing of the upwelling phenomenon.

The strong seasonal cooling and warming of waters observed along the continental margin of the southern Caribbean Sea at the CARIACO station, and particularly in the upper 200 m, is not solely the result of local processes such as radiative cooling, evaporation, and insolation. Instead, temperature changes are largely associated with the replacement of warm surface waters with cooler and more saline subsurface waters through both seasonal wind-driven coastal upwelling and lateral advection. As upwelling subsides, lateral advection of surface water and subduction of subtropical water masses over the region lead to subtropical waters to be located in the 100–150 m depth range again. The period over which this happens, namely July through October, is also associated with increased rainfall and riverine influence (Muller-Karger et al., 1989). However, other regional processes can also affect the hydrography.

Table 1
Depth and concentration of dissolved oxygen minima located above secondary dissolved oxygen maxima associated with ventilation events or "intrusions"

Date	Oxygen minimum depth (m)	Oxygen minimum (μM)	Depth of ventilation peak (m)	Oxygen at ventilation peak (μM)	Depth of deepest Oxygen observed (m)
January 7, 1997	198	23	205	60	
	235	5	245	35	253
June 17, 1997	205	13	215	18	310
August 17, 1997			No peak		300
December 17, 1997	215	8	230	45	300
February 14, 1998			No peak		310
March 12, 1998	280	0	290	14	310
June 9, 1998	190	25	200	43	290
August 5, 1998			No peak		300

Evidence for the role of other processes lies in the interannual variation observed in the hydrography of the upwelling cycle. Early 1997 featured a rapid rise of the 21°C isotherm and the coldest temperatures observed in the series in the upper 100 m (Figs. 2 and 5a). The density structure was different in 1997 relative to 1996 or 1998, with the $26.1\sigma_t$ isopleth rising from 150 m to less than 50 m in approximately 4 months (Fig. 5c). The strong upwelling of 1997 was probably the result of stronger winds early in the season (December–February), the recurrence of strong winds late in the season (April–May), and the most intense secondary summer upwelling observed over the study period. An important consequence was that the first 5 months of 1997 featured higher phytoplankton biomass (3–5 mg m^{-3} in the upper 25 m) and higher average daily primary production (2600 mg C m^{-2} d^{-1}) over a longer period than either 1996 or 1998 (Muller-Karger et al., 2001).

A major change to the "normal" seasonal cycle occurred in 1997–1998, which may have been due to an El Niño-Southern Oscillation (ENSO) event (Nerem et al., 1999; Chavez et al., 1999). The AVHRR record shows higher SST during late 1997 compared to periods before and after that event. This was consistent with changes seen during earlier ENSO events (Enfield and Mayer, 1997; Enfield, 1996). The upward movement of isopleths observed between December and February of 1996 and 1997 was not seen in 1997–1998. In addition, average primary production during the late 1997 to mid-1998 period was 1380 mg C m^{-2} d^{-1}, about half of the values registered during the 1995–1996 and 1996–1997 upwelling periods (Muller-Karger et al., 2001). The wind data were ambiguous and did not confirm the conceptual model (Enfield and Mayer, 1997) of weaker winds in the southern Caribbean during ENSO periods.

A series of events that did not seem related to changes in the wind were observed punctuating the upwelling cycle. Similar short-term features have been documented in other seasonal upwelling regimes (Barton et al., 1977; Codispoti and Friedrich, 1978). While variations in the magnitude of coastal upwelling are mainly due to spatial and temporal variations of the wind, other factors that may be relevant include coastal trapped waves (as seen off Chile by Hormazabal et al., 2001) and eddies migrating along a coast (as seen off the coasts of California and Oregon by Smith, 1995).

In the Cariaco Basin, some very strong upwelling events were associated with subsurface intrusions of Caribbean sea water but not with periods of high winds. The continuous dissolved oxygen profiles provided evidence that punctuated upwelling events were connected to phenomena outside of the Cariaco Basin. Oxygen is supplied only by air–sea gas exchange and photosynthesis in the upper water column, but is used by bacterial respiration processes at all depths. Therefore, the only possible sources of this gas deeper than 200 m at the CARIACO station are downward mixing of surface water or lateral intrusions of oxygenated water from outside the sill. Maxima in oxygen concentration below 200 m (Fig. 7, Table 1) reflected the penetration of "new" water into the Cariaco Basin. Even though the effects of the intrusions were occasionally seen in the discrete (bottle) O_2, nitrate, and pH data (Fig. 8), the continuous O_2 profiles proved to be much more sensitive for detecting these features. It is likely that the subsurface peaks were missed in some of the discrete sample profiles due to wide sample spacing.

The frequency and strength of these ventilation events varied from year to year. Events were detected in January–February, June, August, and December 1997 and in February, March, June, and August 1998 (Table 1, Fig. 7). No events were observed in 1996. Typically, anomalous hydrography associated with an intrusion was observed for 1–3 months following initial detection. The January–February 1997 ventilation was particularly strong (Fig. 7a).

XBT deployed between the CARIACO station and the Cariaco sill (Fig. 1) in December 1997 show a water mass with a temperature range of 19.4–20°C (estimated $\sigma_t = 26.1$) located between 70 and 80 m depth near the Cariaco sill (Fig. 9). The isotherms sloped downward to the south, consistent with the water sinking along this density surface as it penetrated into the Cariaco Basin. If this intrusion moved into the Basin, water above it would have been displaced upward, while oxygen

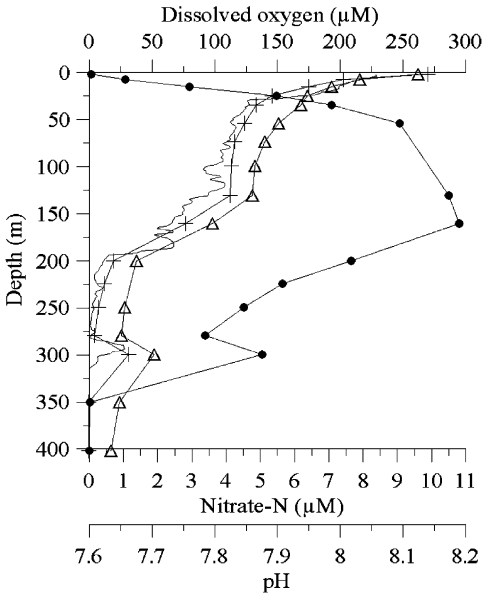

Fig. 8. Vertical distribution of discrete O_2 (μM, +), CTD dissolved oxygen (μM, —), pH (△) and nitrate concentrations (μM, ●) at the CARIACO time-series station during March 1998.

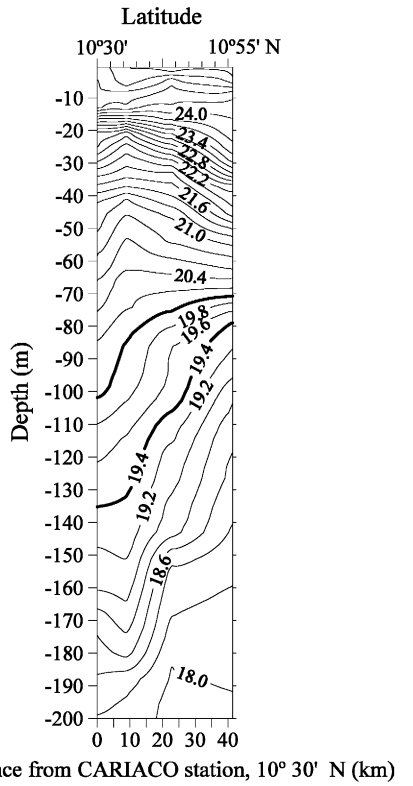

Fig. 9. Vertical distribution of isotherms reconstructed from XBTs deployed on a north–south transect along 64.66°W, north of the CARIACO station, during a ventilation event in December 1997. Contour interval 0.2°C.

would have been injected to depths exceeding 200 m in the central portions of the Basin (Fig. 7).

Deep oxygen maxima were observed well below sill depth in the Cariaco Basin during ventilation events. The oxygen maximum observed in January–February 1997, for example, occurred between 150 and 300 m. The oxic–anoxic interface deepened further (>270 m) during a ventilation event in June 1997 and after the strong earthquake of July 9, 1997 (Thunell et al., 1999; Scranton et al., 2001). The hydrogen sulfide boundary, which was located at 250 m in early 1995, remained below 300 m after mid-1997, probably as a result of the repeated ventilation observed in 1997 (Scranton et al., 2001).

There was also evidence for intrusions in the nitrate and nitrite data. The vertical distribution of nitrite and nitrate (Figs. 5d and e) is strongly influenced by processes of denitrification and nitrification in the Cariaco water column. The primary nitrite maximum near 50 m (Fig. 5e) typically is a result of nitrification. At very low oxygen levels (below about 60 μM), nitrification is less important and bacteria start to use nitrite and nitrate as electron acceptors during respiration. Denitrification takes place, and nitrite and nitrate reach undetectable values. Only an intrusion of oxygenated water can result in additional nitrite or nitrate at intermediate depths. Patches of nitrite up to 0.5 μM were found below 220 m during the ventilation events of January–February 1997, August 1997 and March 1998. Relatively high nitrate levels were also found after the mid-1997 ventilation events. In the Cariaco Basin, below 250 m, hydrogen sulfide typically starts to accumulate at depths where oxygen is undetectable (Richards, 1975) although we have repeatedly observed a region 50–100 m thick where neither oxygen nor sulfide could be measured after periods of intrusion (Scranton et al., 2001).

Ventilation events can have important consequences for phytoplankton at the ocean's surface.

Times of elevated productivity such as seen in January 1997 and in March 1998 were associated with ventilation events (Muller-Karger et al., 2001). During January 1997, productivity was the highest measured for that year, although SST was relatively warm ($\sim 24^{\circ}$C). An uncharacteristically low organic sediment flux was measured in January 1997 (Muller-Karger et al., 2001) and may also have been associated with upward water motion (and therefore particles) as opposed to an increase in respiration of the sinking organic matter. The associated decrease in oxygen between 80 and 150 m in the January–February 1997 event also could have been due to uplift of low oxygen water from below during the intrusion.

Neither the hydrography nor the high surface production associated with the intrusion events was related to changes in local wind intensity. Intrusion events were observed repeatedly and at irregular intervals during 1997 and 1998, even during periods of weak winds. Altimeter SSH anomaly data provided strong evidence that large-scale oceanic phenomena affected the Cariaco Basin. An examination of the gridded SSH anomaly fields for the Caribbean region in 1997 and 1998 revealed a number of eddy features that may have led to the observed ventilations (Fig. 10; Table 2).

Positive SSH anomalies (anticyclonic eddies) were present during January and December 1997 and in June 1998 in the southern Caribbean Sea (Figs. 10a, d and g; Table 2). The anticyclone of January 1997 was centered near 13°N and exhibited a SSH anomaly in excess of 12 cm at its center. Its edge (2 cm boundary) was located immediately off the Cariaco sill. In December 1997, an anticyclone occupied the entire eastern/central Caribbean Sea with a strong positive SSH anomaly of >12 cm at its center. The eddy was approximately $680 \times 300\,\mathrm{km}^2$ in size, with the major axis aligned from southeast to northwest, and the southeastern boundary was located near the shelf outside the Cariaco Basin. The anticyclone of June 1998 was centered near 66°W and was also located near the Cariaco shelf.

Negative SSH anomalies (cyclonic eddies) occurred during June and August 1997, and February, March and August 1998 (Figs. 10b, c, e, f and h; Table 2). In June 1997 a cyclone was located immediately off the shelf north of Cariaco with SSH anomaly <-14 cm at its center. In August 1997, presumably the same eddy was found some 100 km to the west at 13°N, with a SSH anomaly at its center of <-12 cm and its boundary overlapping the Cariaco sill. During February 1998, a cyclone with a -20 cm SSH anomaly at its center was observed off the Venezuelan shelf near 67°W. It is assumed that this cyclone passed near the Cariaco Basin in January or early February 1998. This feature moved to around 72°W by March, while another strong cyclone entered the southeastern Caribbean from the Atlantic Ocean. In August 1998, a cyclone was centered near 13.5°N and 67°W with its southern boundary near the shelf off Cariaco.

Eddies detected using satellite altimetry in the Caribbean Sea have been discussed in several previous studies (Nystuen and Andrade, 1993; Carton and Chao, 1999; Pauluhn and Chao, 1999; Murphy et al., 1999; Andrade and Barton, 2000). Indeed, the data shown in Pauluhn and Chao (1999) reflects the two eddies we detected in the first half of 1997. Andrade and Barton (2000) demonstrated that anticyclones and cyclones observed in the Venezuela Basin may originate either locally within the Basin or enter the Caribbean Sea through the Antillean passages. However, previous studies have largely focused on the central and northern Caribbean in an effort to understand the transfer of energy and water from the equatorial to the subtropical Atlantic, and have provided little insight as to the impact of these features on the hydrography of Venezuelan margin and particularly the effect on continental margin processes.

The hydrographic results (Table 1) combined with the SSH data (Fig. 10, Table 2) suggested that the punctuated (non-seasonal) ventilation events within the basin were the result of the interaction of anticyclonic or cyclonic eddies in the Venezuela Basin with the continental shelf and the Cariaco sill. Every ventilation event observed in the Cariaco Basin in 1997 and 1998 (Table 1) was associated with an eddy near the shelf in the southeastern Caribbean (Fig. 10, Table 2). While there were eddies detected in the Caribbean with the TOPEX observations in 1996, the number and

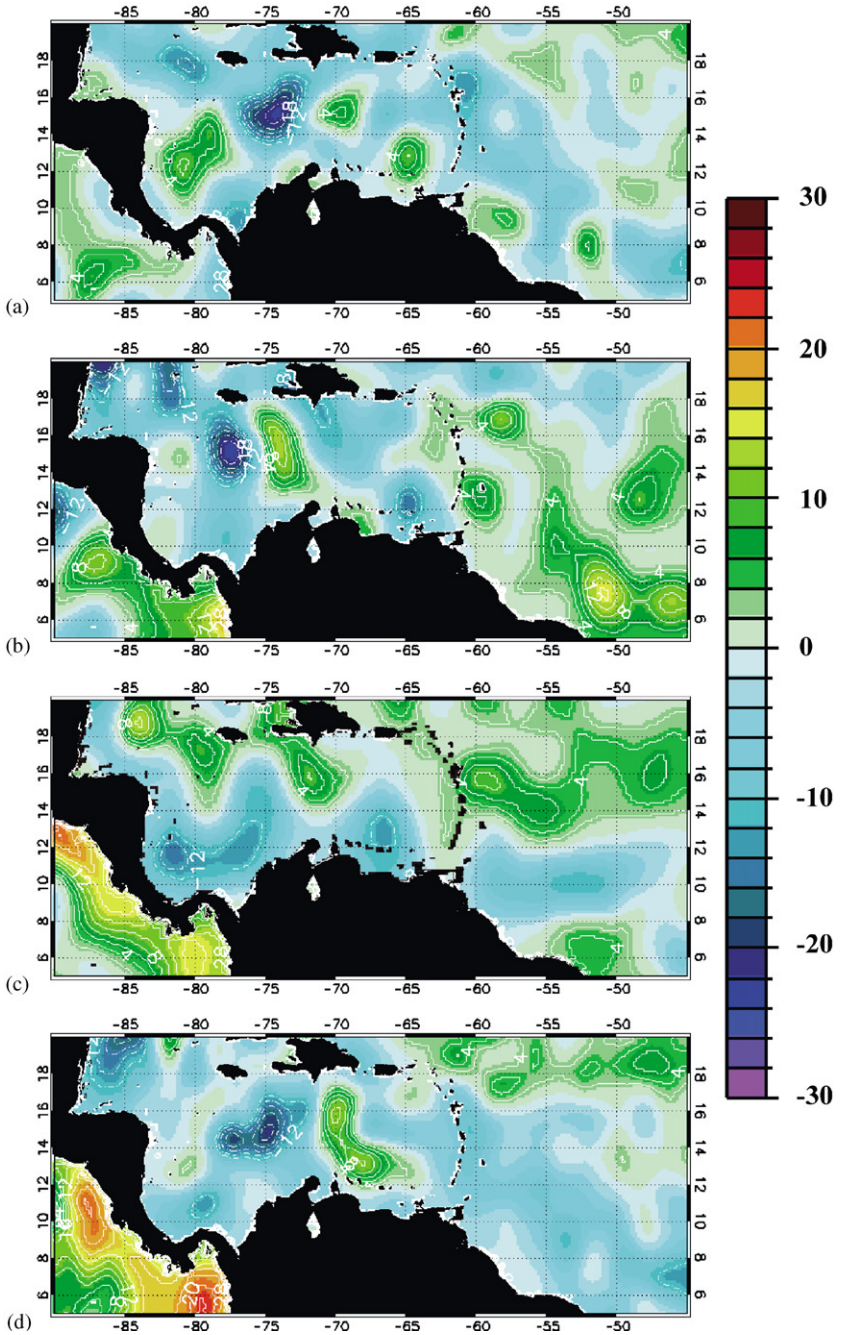

Fig. 10. Satellite-derived sea surface height (SSH) anomaly maps (cm) of the Caribbean region. Panels a, b, c and d correspond to January, June, August and December 1997, respectively. Panels e, f, g and h correspond to February, March, June and August 1998. Contours trace cyclonic (negative, broken lines) and anticyclonic (positive, solid lines) eddies. Positive contours start at 2 cm and negative ones start at –12 cm, each with a 2 cm contour increment or decrement; SSH anomaly (cm) has been scaled to match the color bar provided.

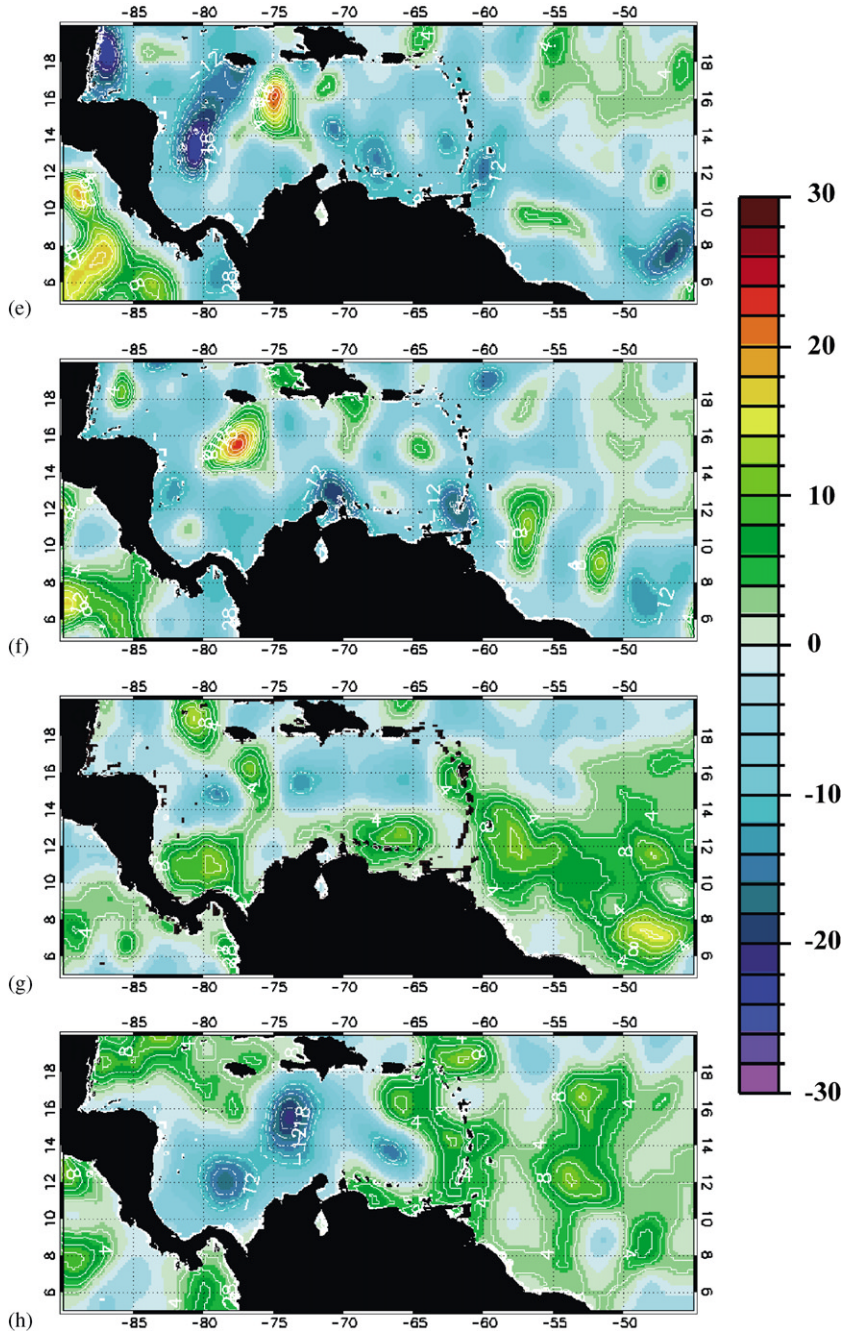

Fig. 10 (*continued*).

SSH anomaly strength seemed to be smaller than what was observed in 1997 and 1998. In 1996 only three eddy events were detected on the southern margin of the Caribbean, near the Cariaco Basin. Of these, only the anticyclonic event of October 1996 was of substantial proportion, with the eddy

Table 2
Eddies observed in the southeastern Caribbean (see also Fig. 10). Center SSHA is the approximate sea surface height anomaly near the center of the eddy as estimated by the TOPEX/Poseidon satellite altimeter

Date	Eddy type	Center location	Center SSHA (cm)	Diameter (km)	Figure
March 1996	Cyclone	12.5°N, 64.5°W	<-16	100	
October 1996	Anticyclone	13.0°N, 65.0°W	>12	200	
December 1996	Anticyclone	13.0°N, 65.0°W	>12	100	
January 1997	Anticyclone	13.0°N, 65.0°W	>12	210	10a
June 1997	Cyclone	12.5°N, 64.5°W	<-14	170	10b
August 1997	Cyclone	13.0°N, 66.5°W	<-12	170	10c
December 1997	Anticyclone	12–17°N, 65–72°W	>12	680×300	10d
February 1998	Cyclone	13.0°N, 68.0°W	-20	285	10e
March 1998	Cyclone	12.0°N, 62.0°W	<-12	190	10f
June 1998	Anticyclone	12.5°N, 66.0°W	>8	247×470	10g
August 1998	Cyclone	13.0°N, 67.0°W	<-14	170	10h

exceeding 200 km in diameter and 12 cm SSH anomaly near its center. A cyclone seen in March and an anticyclone seen in December 1996 were, however, small in diameter (order of 100 km) relative to the eddies that would be seen later in 1997 and 1998. The small size of these eddies combined with the lack of ventilations suggested that there were no major impacts by eddies on the hydrography of the Cariaco Basin in 1996.

In the particular instance of February and March 1998, two intense cyclonic eddies (Figs. 10e and f) were located off central Venezuela on either side of the Cariaco Basin. It is not clear that such eddies always propagated to the west. These particular eddies did not appear to move in subsequent weekly altimeter SSH anomaly renditions and appeared to dissipate locally. In the period between September and December 1998, no ventilation events were observed and only weak and unorganized anticyclonic activity was apparent in the eastern Caribbean. Normal conditions (no ventilation) were always associated with the absence of eddies in the region.

The particular physical characteristics of an eddy may determine the way it interacts with the shelf and the effect on the hydrography within the Cariaco Basin. The anticyclones seemed to inject water at mid-depth, pushing water upwards. The presence of cyclones north of 12°N, as in August 1997, February 1998, and August 1998, seemed to be associated with a ventilation event leading to higher oxygen concentrations in the upper 350 m, but no clear subsurface intrusion peak.

Anticyclonic eddies feature depressed isopycnals associated with the thermocline at their center and raised isopycnals along their boundaries. Also, the pressure gradient force for an anticyclonic eddy is directed radially outward. As such an eddy encounters a slope, the mechanism of the bottom Ekman layer will drive fluid up slope under the area of an eddy, featuring a strong current and strong pressure gradient (R. Weisberg, personal communication). Rubbing of the eddy on the slope creates an Ekman layer in which the flow slows down and the radially outward pressure gradient force drives fluid toward the sill against a reduced Coriolis force (reduced because the fluid is slowed by friction). We unfortunately have no data to verify this conceptual model or make inferences about the kinematics of the bottom boundary layer, but the larger impact on ventilation in the vicinity of the sill may be due primarily to the elevated isopycnals around the periphery of the eddy. When the boundaries of such an eddy approach the shelf break, cold and dense Caribbean Sea water located below the level of the SUW may be drawn up onto the shelf, move over the Cariaco sill, and sink within the Cariaco Basin. Such waters would spread at their level of vertical stability introducing oxygen and nitrate-rich water to intermediate depths of the Cariaco Basin.

Cyclonic eddies, on the other hand, have raised thermocline-related isopycnals in the interior relative to the border of the eddy. Their interaction with the Venezuelan shelf effectively would lead to downwelling near the Cariaco Basin sill and a depression of isopycnals within the Cariaco Basin. It is possible that such downwelling may lead to a spill of saline but warmer waters over the Cariaco sill.

The nutrient pumping effect observed as these eddies approach the Cariaco Basin represents a mechanism which will supply nutrients along the entire continental margin of the southern Caribbean Sea, thereby enhancing regional primary production. These processes, however, are poorly understood. It will only be through systematic, in situ time series observations such as those conducted at the CARIACO station that we will understand their impact on carbon fluxes and long-term ocean processes.

Acknowledgements

The National Science Foundation (NSF Grants OCE-9729284 and OCE-9216626 to FMK and OCE-9415790, OCE-9711318, and OCE-9730278 to MIS and Gordon Taylor) and the Consejo Nacional de Investigaciones Cientificas y Tecnologicas (CONICIT, VENEZUELA, Grant 96280221) supported this work. We are indebted to the personnel of the Fundacion La Salle de Ciencias Naturales, Estacion de Investigaciones Marinas Isla Margarita (FLASA/EDIMAR) for their enthusiasm and professional support. In particular, we thank Dr. Pablo Mandazen (Hermano Gines, Director, FLASA) for his confidence in our activities, and the crew of the *R/V Hermano Gines* (FLASA) for their able support at sea. Ramon Varela provided unwavering leadership in coordinating and carrying out field expeditions. Jonnathan Garcia, Javier Gutierrez, Anadiuska Rondon (all at FLASA/EDIMAR), and Richard Bohrer, John Akl and Ana Lucia Odriozola (at USF) provided essential field and laboratory support. Luis Troccoli, Wilfredo Patiño, Luis Sanchez, and William Senior, from the Universidad de Oriente, Cumana, Venezuela, and Kent Fanning from the University of South Florida provided nutrient data. Lucy Fitzgerald Smedstad from Naval Research Laboratory at Stennis Space Center provided the gridded TOPEX/Poseidon data. We thank Robert Weisberg (at USF) for sharing his insight into eddy–topography interactions with us. State University of New York Marine Sciences Research Center contribution number 1241. USF Institute for Marine Remote Sensing contribution number 40.

References

Aminot, A., 1983. Dosage de l'oxygène dissous. In: Aminot, A., Chaussepied, M. (Eds.), Manuel de Analyses Chimiques en Milieu Marin. Centre National pour L'Exploitation des Oceans, CNEXO, France, pp. 75–92.

Andrade, C.A., Barton, E.D., 2000. Eddy development and motion in the Caribbean Sea. Journal of Geophysical Research. 105 (C11), 26191–26201.

Astor, Y., Meri, J., Muller-Karger, F., 1998. Variabilidad estacional hidrográfica en la Fosa de Cariaco. Memorias Sociedad. Ciencias. Naturales. La Salle 53 (149), 61–72.

Barton, E.D., Huyer, A., Smith, R., 1977. Temporal variation observed in the hydrographic regime near Cabo Corveiro in the northwest African upwelling region, February to April 1974. Deep-Sea Research 24, 7–23.

Black, D.E., Peterson, L.C., Overpeck, J.T., Kaplan, A., Evans, M.N., Kashgarian, M., 1999. Eight centuries of North Atlantic Ocean atmosphere variability. Science 286, 1709–1713.

Carton, J.A., Chao, Y., 1999. Caribbean Sea eddies from TOPEX/POSEIDON altimetry and a 1/6° Atlantic Ocean model simulation. Journal of Geophysical Research 104 (C4), 7743–7752.

Chavez, F.P., Strutton, P.G., Friedrich, G.E., Feely, R.A., Feldman, G.C., Foley, D.G., McPhaden, M.J., 1999. Biological and chemical response of the Equatorial Pacific Ocean to the 1997–80 El Niño. Science 286, 2126–2131.

Clayton, T.D., Byrne, R.H., 1993. Spectrophotometric seawater pH measurements: total hydrogen ion concentration scale calibration of m-cresol purple and at-sea results. Deep-Sea Research Part 1 40 (10), 2115–2129.

Codispoti, L.A., Friedrich, G.E., 1978. Local and mesoscale influences on nutrient variability in the northwest African upwelling region near Cabo Corbeiro. Deep-Sea Research 25, 751–770.

Enfield, D.B., 1996. Relationships of inter-American rainfall to tropical Atlantic and Pacific SST variability. Geophysical Research Letters 23, 3305–3308.

Enfield, D.B., Mayer, D.A., 1997. Tropical Atlantic sea surface variability and its relation to El Niño-southern oscillation. Journal of Geophysical Research 102 (C1), 929–945.

Gordon, L.I., Jennings Jr., J.C., Ross, A.A., Crest, J.M., 1993. A suggested protocol for continuous flow automated analysis of seawater nutrients. In: WOCE Operation Manual. WHP Office Report 90-1, WOCE Report 77, No. 68/91. Woce Hydrographic Program Office, Scripps Institution of Oceanography, La Jolla, CA, pp. 1–52.

Haug, G., Pedersen, T., Sigman, D., Calvert, S., Nielsen, B., Peterson, L., 1998. Glacial/interglacial; variations in production and nitrogen fixation in the Cariaco Basin during the last 580 kyr. Paleoceanography 13, 427–432.

Herrera, L., Febres-Ortega, G., 1975. Procesos de surgencia y renovación de aguas en la Fosa de Cariaco, Mar Caribe. Boletín del Instituto Oceanográfico de la Universidad de Oriente 14 (1), 31–44.

Hormazabal, S., Shaffer, G., Letelier, J., Ulloa, O., 2001. Local and remote forcing of sea surface temperature in the coastal upwelling system off Chile. Journal of Geophysical Research 106 (C8), 16657–16671.

Hughen, K., Overpeck, J., Peterson, L., Trumbore, S., 1996. Rapid climate changes in the tropical Atlantic region during the last glaciation. Nature 380, 51–54.

Hughen, K.A., Overpeck, J.T., Lehman, S.J., Kashgarian, M., Southon, J., Peterson, L.C., Alley, R., Sigman, D.M., 1998. Deglacial changes in ocean circulation from an extended radiocarbon calibration. Nature 391, 65–68.

McClain, E.P., Pichel, W.G., Walton, C.C., Ahmad, Z., Sutton, J., 1983. Multi-channel improvements to satellite-derived global sea-surface temperatures. Advances in Space Research 2 (6), 43–47.

Morrison, J.M., Smith, O.P., 1990. Geostrophic transport variability along the Aves ridge in the Eastern Caribbean Sea during 1985 and 1986. Journal of Geophysical Research 95, 699–710.

Muller-Karger, F.E., Aparicio, R., 1994. Mesoscale processes affecting phytoplankton abundance in the southern Caribbean Sea. Continental Shelf Research 14, 199–221.

Muller-Karger, F.E., McClain, C.R., Fisher, T.R., Esaias, W.E., Varela, R., 1989. Pigment distribution in the Caribbean Sea: observations from space. Progress in Oceanography 23, 23–69.

Muller-Karger, F., Varela, R., Thunell, R., Scranton, M., Bohrer, R., Taylor, G., Capelo, J., Astor, Y., Tappa, E., Ho, T.-Y., Iabichella, M., Walsh, J.J., Diaz, J.R., 2000. Sediment record linked to surface processes in the Cariaco basin. EOS, Transactions, American Geophysical Union 81(45), 529, 534–535.

Muller-Karger, F.E., Varela, R., Thunell, R., Scranton, M., Bohrer, R., Taylor, G., Capelo, J., Astor, Y., Tappa, E., Ho, T-Y., Walsh, J.J., 2001. Annual cycle of primary production in the Cariaco Basin: response to upwelling and implications for vertical export. Journal of Geophysical Research 106 (C3), 4527–4542.

Murphy, S.J., Hurlburt, H.E., O'Brien, J.J., 1999. The connectivity of eddy variability in the Caribbean Sea, the Gulf of Mexico, and Atlantic Ocean. Journal of Geophysical Research. 104 (C1), 1431–1453.

Nerem, R.S., Chambers, D.P., Leuliette, E.W., Mitchum, G.T., Giese, B.S., 1999. Variations in global mean sea level associated with the 1997–1998 ENSO event: implications for measuring long-term sea level change. Journal of Geophysical Research 26 (19), 3005–3008.

Nystuen, J.A., Andrade, C., 1993. Tracking mesoscale ocean features in the Caribbean Sea using Geosat altimetry. Journal of Geophysical Research 98 (C5), 8389–8394.

Pauluhn, A., Chao, Y., 1999. Tracking eddies in the subtropical north-western Atlantic Ocean. Physical Chemistry. Earth (A) 24 (4), 415–421.

Peterson, L.C., Overpeck, J.T., Kipp, N.G., Imbrie, J., 1991. A high-resolution late quaternary upwelling record from the anoxic Cariaco Basin, Venezuela. Paleoceanography 6, 99–119.

Pouliquen, S., Harscoat, M.V., Bentamy, A., 1996. WNF Products—User Manual. Reference No. C2-MUT-W-01-IF. IFREMER/CERSAT, Plouzané, France. 57 pp.

Richards, F.A., 1960. Some chemical and hydrographic observations along the north coast of South America. I. Cabo Tres Puntas to Curacao, including the Cariaco Trench and the Gulf of Cariaco. Deep-Sea Research 7, 163–182.

Richards, F.A., 1975. The Cariaco Basin (Trench). Oceanography and Marine Biology Annual Review 13, 11–67.

Richards, F.A., Vaccaro, R.F., 1956. The Cariaco Trench, an anaerobic basin in the Caribbean Sea. Deep-Sea Research 3, 214–228.

Scranton, M.I., Sayles, F.L., Bacon, M.P., Brewer, P.G., 1987. Temporal changes in the hydrography and chemistry of the Cariaco Trench. Deep-Sea Research 34, 945–963.

Scranton, M.I., Astor, Y., Bohrer, R., Ho, T.-Y., Muller-Karger, F.E., 2001. Controls on temporal variability of the geochemistry of the deep Cariaco Basin. Deep-Sea Research, Part 1 48, 1605–1625.

Smith, R.L., 1995. The physical process of coastal ocean upwelling systems. In: Summerhayes, C.P., Emeis, K-C., Angel, M.V., Smith, R.L., Zeitzschel, B. (Eds.), Upwelling in the Ocean: Modern Processes and Ancient Records. Wiley, England, pp. 39–64.

Strickland, J.D.H., Parsons, T.R., 1972. A Practical Handbook of Seawater Analysis, 2nd Edition. Fisheries Research Board of Canada, Bulletin 167, National Research Council Canada, Ottawa, 310pp.

Thunell, R., Tappa, E., Varela, R., Llano, M., Astor, Y., Muller-Karger, F., Bohrer, R., 1999. Increased marine sediment suspension and fluxes following an earthquake. Nature 398, 233–236.

Thunell, R., Varela, R., Llano, M., Collister, Muller-Karger, J.F., Bohrer, R., 2000. Organic carbon fluxes, degradation, and accumulation in an anoxic basin: sediment trap results from the Cariaco Basin. Limnology and Oceanography 45(2), 300–308.

Walsh, J.J., Dieterle, D.A., Muller-Karger, F.E., Bohrer, R., Bisset, W.P.t, Varela, R.J., Aparicio, R., Díaz, R., Thunell, R., Taylor, G.T., Scranton, M.I, Fanning, K.A, Peltzer,

E.T., 1999. Simulation of carbon–nitrogen cycling during spring upwelling in the Cariaco Basin. Journal Geophysical Research 104 (C4), 7807–7825.

Wust, G., 1964. Stratification and Circulation in the Antillean-Caribbean basins. Part 1. Spreading and Mixing of the Water Types. Columbia University Press, New York, 201 pp.

Yarincik, K., Murray, R., Peterson, L., 2000. Climatically sensitive eolian and hemipelagic deposition in the Cariaco Basin, Venezuela, over the past 580,000 years: results from Al/Ti and K/Al. Paleoceanography 15, 210–228.

Zhang, J., Millero, F.J., 1993. The chemistry of the anoxic waters in the Cariaco Trench. Deep-Sea Research Part 1 40 (5), 1023–1041.